Eur Biophys J (2008) 37:469–481
DOI 10.1007/s00249-007-0239-y

ORIGINAL PAPER

Studies of distribution, location and dynamic properties of EGFR on the cell surface measured by image correlation spectroscopy

Eleonora Keating · Anja Nohe · Nils O. Petersen

Received: 16 March 2007 / Revised: 11 October 2007 / Accepted: 28 October 2007 / Published online: 28 November 2007
© EBSA 2007

Abstract In this work, we have studied the distribution and dynamic properties of Epidermal Growth Factor (EGF) receptors in the plasma membrane of fixed and live cells as well as the extent of co-localization of this transmembrane protein with proteins specific for three-membrane microdomains: membrane rafts, caveolae and clathrin-coated pits. This was achieved using a family of image-processing tools called image correlation spectroscopy (ICS), image cross-correlation spectroscopy (ICCS) and dynamic image correlation spectroscopy (DICS). Our results indicate that EGFR is diffusely distributed on the cell surface at 37°C and aggregates as the temperature is lowered to 4°C. This aggregation takes place within 15 min and is reversible. Changes in temperature also affect the diffusion of EGFR by two orders of magnitude. The dynamic properties of EGFR are similar to the dynamic properties of a GPI-anchored protein known to be present in membrane rafts, which motivated us to explore the extent of co-localization of EGFR with this membrane raft protein using ICCS. Our results indicate that more than half of the EGFR population is present in membrane rafts and smaller percentages are present in caveolae and clathrin-coated pits.

E. Keating · N. O. Petersen
Department of Chemistry, The University of Western Ontario, London, ON, Canada

A. Nohe
Department of Chemical Engineering and Institute for Molecular Biophysics, University of Maine, Orono, ME, USA

N. O. Petersen (✉)
National Institute for Nanotechnology, National Research Council Canada, Edmonton, AB, Canada
e-mail: Nils.Petersen@nrc-cnrc.gc.ca

Keywords EGFR · Diffusion · Plasma membrane microdomains · Membrane rafts · Temperature dependence · Image correlation spectroscopy

Introduction

The plasma membrane of cells is a chemically and physically heterogeneous environment where specific protein–protein and lipid–lipid interactions lead to the formation of domains in the cell membrane. These domains vary in size, composition and function. Some domains are characterized by the presence of a particular protein while others have an increased concentration of a specific lipid. Examples of membrane microdomains that have been extensively studied are membrane rafts, caveolae and clathrin-coated pits. Membrane rafts and caveolae are domains that are enriched in cholesterol and glycosphingolipids and play crucial roles in a large number of cellular functions such as cell signaling and endocytosis (Brown 1992; Fiedler et al. 1993; Prinetti et al. 2000). Caveolae, believed to be a subset of membrane rafts, are 50–100 nm invaginations in the cell membrane that are additionally enriched in the protein caveolin (Harder and Simons 1997; Parton and Simons 1995). Clathrin-coated pits are also invaginations in the cell membrane that are important in endocytosis (Schmid 1997). These domains are characterized by the presence of two proteins: clathrin and the clathrin-associated adaptor protein, AP-2.

The epidermal growth factor receptor (EGFR) is a transmembrane glycoprotein with intrinsic tyrosine kinase activity that belongs to the erbB family (Ullrich et al. 1984). The information transfer is initiated by ligand-binding which leads to receptor dimerization of the receptor either with itself or with other members of the

erbB family. The EGFR signal is inactivated through endocytosis of the receptor-ligand complex. Extensive research has been done to determine the location of EGFR on the cell surface prior to and following ligand binding. EGFR has been shown to directly interact with AP-2 (Sorkin et al. 1996) as well as caveolin-1 (Couet et al. 1997) via specific amino acid motifs in the receptor cytoplasmic domain. EGF receptors have been shown to be internalized via clathrin-coated pits (Carpentier et al. 1982; Gorden et al. 1978; Hanover et al. 1984) as well as clathrin-independent processes (Haigler et al. 1979; Hopkins et al. 1985). It has been proposed that caveolae are the main sites of EGFR signaling based on results that demonstrate that caveolin-1 and EGFR both co-localize to low density, carbonate-insoluble membrane regions (Couet et al. 1997; Liu et al. 1996; Mineo et al. 1996; Pike and Miller 1998). However, caveolin-1 and EGFR can be separated by differences in solubility in nonionic detergent (Waugh et al. 1999). Studies using immunoelectron microscopy have shown that only a small fraction of EGFR is in caveolae, further suggesting that EGFR is mainly localized in non-caveolar membrane domains, such as membrane rafts (Ringerike et al. 2002). Other studies have also reported that EGFR are enriched in membrane rafts (Mineo et al. 1996; Pike and Miller 1998).

Cell membranes are not only heterogeneous in nature but also dynamic. Experimental evidence has shown that proteins are not free to diffuse within the cell membrane (Sheets et al. 1995). One area of widespread interest is how membrane microdomains affect protein's ability to laterally diffuse in the cell membrane. Some proteins are confined in domains for a certain period of time then are free to diffuse. Other proteins are trapped within domains set up by the membrane-associated cytoskeleton, which is a lattice-like network of filamentous proteins. Proteins can escape as the distance between the cytoskeleton and the cell membrane fluctuates over time. Proteins that directly interact with the cytoskeleton can undergo directed motion while other proteins are known to undergo free random diffusion. Measurements of the lateral mobility of membrane proteins such as receptors will enable us to better understand the dynamic processes that take place in the membrane plane which are important in understanding a variety of cellular processes. For example, during receptor-mediated endocytosis, receptors diffuse to coated pits, or other endocytic domains, before internalization (Goldstein et al. 1985). Similarly, transduction of many signals from outside the cell depends on receptors diffusing to form dimers or trimers as a result of binding extracellular ligands (Schlessinger 1986; Metzger 1992).

The objective of this work was to determine the distribution, dynamic properties and location of EGFR clusters on the surface of cells. We achieved this by using fixed and live cells fluorescently labeled for proteins of interest. High-magnification images were collected at the cell surface, which were analyzed by a family of image processing tools called image correlation spectroscopy. Our results show that EGFR is diffusely distributed on the cell surface at 37°C and aggregates as the temperature is lowered to 4°C. This aggregation takes place within 15 min and is reversible. EGFR clusters are dynamic at 37°C and undergo free as well as restricted diffusion as observed by visual analysis of confocal images collected over a few minutes. Lowering the temperature also affects the diffusion of EGFR by two orders of magnitude. The dynamic properties of EGFR are similar to those of a GPI-anchored protein shown to be present in membrane rafts. Our results indicate that more than half of the EGFR population is present in membrane rafts and smaller percentages are present in caveolae and clathrin-coated pits.

Materials and methods

Cell culture

Green African monkey fibroblast cells (COS-7) and human epidermoid carcinoma (A431) cells were obtained from American Type Culture Collection (Rockville, MD, USA). COS-7 and A431 cells were cultured in high glucose (4 g/l D-glucose) Dulbecco's modified eagle medium (DMEM) supplemented with 10% fetal bovine serum (FBS) and antibiotics, penicillin (50 IU/ml) and streptomycin (100 μg/ml). The cells were maintained in a humidified incubator at 37°C and 5% CO_2 and were passaged approximately every 3 days to maintain exponential growth.

Fixing and immunostaining cells

Cells were rinsed with cold PBS prior for being fixed. For the temperature dependence of the EGFR distribution studies, cells were maintained at the desired temperature in media for a set length of time and then fixed with 4.4% paraformaldehyde in PBS at the experimental temperature for 20 min. In all other cases, cells were fixed for 5 min in cold methanol at −20°C followed by 2 min in cold acetone at −20°C.

Prior to immunostaining, cells were washed twice with PBS and once with PBS containing 2% BSA. For immunolabeling of EGFR in the temperature-dependent experiments, a mouse monoclonal antibody (clone 29.1; Sigma, St. Louis, MO, USA) was used in conjunction with goat anti-mouse AF488 (Molecular Probes, Eugene, OR, USA). In all other experiments, EGFR was immunolabeled

using a polyclonal goat antibody (clone 1005) in conjunction with donkey anti-goat AF568 (Molecular Probes, Eugene, OR, USA). Immunostaining of AP-2 was achieved using a mouse monoclonal antibody, AC1-M11. AC1-M11 was a kind gift from Dr. Margaret S. Robinson (University of Cambridge, Cambridge, UK) and is specific for the αa and αc chains of AP-2 (Robinson 1987). Two monoclonal antibodies were used to immunolabel the α and β isoforms of caveolin-1 (BD Transduction Laboratories, Mississauga, ON, Canada). Clone 2234 is specific for the α isoform of caveolin-1 while clone 2297 recognizes both α and β isoforms. Fluorescently tagged secondary antibody was goat anti-mouse AF488. Normal goat IgG (Sigma, St. Louis, MO, USA) was used to block non-specific binding. All antibody incubations were carried out at room temperature for 30 min. Between antibody incubations, cells were washed twice with PBS and once with PBS containing 2% BSA for 5–10 min each time while being agitated on a tilt table (Wave-Master, Vantronics, London, ON, Canada). In co-localization experiments, EGF-stimulated A431 cells were obtained by incubating cells with 37.5 ng/ml EGF for 10 min at 37°C. This incubation time was chosen since incubating cells with the same concentration of EGF at 37°C for 3, 5, 10 and 20 min showed no difference in the number of EGFR at the cell surface (results not shown). Coverslips were mounted on microscope slides using Airvol mounting media (containing n-propylgallate) and stored at 4°C in the dark. All antibodies were used at saturating concentrations as determined using ICS measurements (St Pierre and Petersen 1992).

Cell transfection

For the diffusion measurements, COS-7 cells were transiently transfected with the appropriate plasmid DNA using FuGENE6 Transfection Reagent (Roche, Mississauga, ON, Canada) according to manufacturer's protocol. ErbB1-GFP was a kind gift from Dr. Arndt-Jovin (Max Planck Institute for Biophysical Chemistry, Gottingen, Germany). The fusion protein was inserted into pEGFP-N1 from Clontech (Mountain View, CA, USA) (Nagy et al. 2003). For simplicity, ErbB1-GFP will be referred to as EGFR-GFP throughout this paper. The plasmids encoding caveolin-1α-GFP and caveolin-1β-GFP were provided by Dr. H. Kogo (Department of Anatomy, Nagoya University School of Medicine, Showa-ku, Nagoya 466–8550, Japan). The plasmid encoding the beta subunit of AP-2 was obtained from Dr. Steve Furguson (Roberts Research Institute, London, ON, Canada).

For the co-localization studies of EGFR and a GPI-anchored protein, A431 cells were transiently transfected with the GFP-GL-GPI DNA using FuGENE6 Transfection Reagent. GFP-GL-GPI is a fusion protein containing the signal sequence of rabbit lactase phlorizin hydrolase (LPH), an N-glycosylation site thought to be important for proper targeting and the GPI-attachment signal of LFA-3 (Pralle et al. 2000). This plasmid DNA was kindly provided by Dr. Gisou van der Goot (University of Geneva, Geneva, Switzerland) with permission from Dr. Patrick Keller (MPI, Dresden, Germany). For simplicity, GFP-GL-GPI DNA will be referred to as GPI-GFP DNA throughout. All transfections were performed on cells grown in 35-mm diameter dishes using 3 μg of DNA per plasmid construct and 7 μl of FuGENE6 diluted in DMEM supplemented with antibiotic without FBS.

Diffusion measurements

The diffusion properties of EGFR, AP-2 and caveolin-1 in cell membranes were measured on live COS-7 cells, 48 h after trasfection. The temperature was regulated with a Cambion Bipolar temperature controller (Cambion Division of Midland Ross, Brampton, ON, Canada) with a microscope stage subassembly. The cells were maintained under DMEM supplemented with antibiotics without FBS. The temperature of the sample was monitored with an external thermometer accurate to within ±1°C.

Confocal microscopy

Images were collected using a BioRad MRC 600 confocal microscope equipped with an Ar/Kr mixed gas laser and an inverted Nikon microscope. Total laser power is 25 mW and images were collected at 1% laser power by attenuating with neutral density filters. GFP and AF488 were visualized by excitation at 488 nm while AF568 was visualized by excitation at 568 nm. In the case when two fluorophores were used, AF488 or GFP emission was collected first from photomultiplier tube 2 and then AF568 emission was collected from photomultiplier tube 1. The confocal pinhole was set to position 8 on the instrument's vernier scale (corresponding to a confocal pinhole diameter of 4.2 mm). The black level was maintained at 6.0 on the vernier scale and the gain was set at 10.0 (maximum).

Fluorescent cells were localized using a 60× immersion objective and mercury lamp illumination. Images suitable for ICS analysis were collected from the periphery of the cell in photon-counting mode to ensure linear amplification of the intensity signal. These images were collected using a zoom factor of 10, as square images with 512 × 512 pixels, corresponding to a pixel resolution of 0.032 μm in the x and the y direction. Between 5 and 10, scans were accumulated to produce a single image. One image was

collected per cell and 35 to 40 images from individual cells were analyzed per experiment. For the diffusion studies, a time series of 50 images was collected from the same area of a cell with 8 or 15-s delay time between images (depending on protein). Sets of images from 10 to 30 cells were obtained for each experimental condition.

A "white noise" background image (Wiseman and Petersen 1999) was obtained at the beginning and at the end of each set of images by initiating image acquisition with the light path to the sample blocked.

Image correlation spectroscopy (ICS) and image cross-correlation spectroscopy (ICCS)

Image correlation spectroscopy (ICS) is based on analysis of spatial intensity fluctuations in images collected on a confocal laser-scanning microscope (Petersen et al. 1993; Wiseman 1995). Autocorrelation functions, $g(\xi,\eta)$, were calculated as described earlier (Petersen et al. 1993; Wiseman 1995) and were fit to a two-dimensional Gaussian function as in Eq. 1

$$g(\xi,\eta) = g(0,0)\mathrm{e}^{(\xi^2+\eta^2)/\omega^2} + g_0 \tag{1}$$

where ξ and η are the position lag coordinates (for the x and y axes, respectively) of the autocorrelation function, ω is the e^{-2} radius of the laser beam, and the $g(0,0)$ is the amplitude of the autocorrelation function upon extrapolation of ξ and η to zero; the offset, g_0, is introduced to account for the finite sample of the images, which can result in a decay of $g(\xi,\eta)$ to a non-zero level at large lag coordinates. The zero-lag amplitude of the autocorrelation function, $g(0,0)$, has been shown to be inversely proportional to the number of independently distributed particles in the observation area (Petersen 1986):

$$g(0,0) = \frac{1}{\overline{N}_p} \tag{2}$$

A cluster density (CD) value, which is defined as the average number of independent fluorescent particles per μm^2 of cell membrane, can be calculated as shown below:

$$\mathrm{CD} = \frac{1}{g(0,0)\pi\omega^2} \tag{3}$$

The average intensity of an image, $\langle i(x,y)\rangle$, is proportional to the average number of fluorescent molecules in the area illuminated by the laser beam. Thus, the degree of aggregation (DA) can be calculated, which is defined as the average number of molecules in the protein aggregate and is obtained by dividing the average total number of protein monomers, $\overline{N}_m$, by the average number of independent protein particles, $\overline{N}_p$, according to Eq. 4:

$$\mathrm{DA} = \langle i(x,y)\rangle g(0,0) = c\frac{\overline{N}_\mathrm{m}}{\overline{N}_\mathrm{p}} \tag{4}$$

The constant c accounts for instrumental and experimental parameters (extinction coefficients, quantum yields and efficiency of collection of the confocal microscope). These parameters are constant for a given set of experimental conditions. In this work, the constant c is not known and therefore, all reported DA values are relative values.

Image cross-correlation spectroscopy (ICCS) is a member of the ICS family and is used to study the spatial correlation between two spectrally separated labels (Brown 1998; Petersen et al. 1998; Rocheleau and Petersen 2000; Srivastava and Petersen 1996; Srivastava 1998). In addition to the autocorrelation analysis, a cross-correlation function can be calculated. The zero-lag amplitude of this function, $g_{gr}(0,0)$, has been shown to reflect the extent of co-localization of two chromophores [for simplicity the two chromophores are referred to as green (g) and red (r)] (Brown 1998; Petersen et al. 1998; Rocheleau and Petersen 2000; Srivastava and Petersen 1996; Srivastava 1998):

$$\begin{aligned}\lim_{\xi\to 0,\eta\to 0} g_{\mathrm{gr}}(\xi,\eta) = g_{\mathrm{gr}}(0,0) &= \frac{\overline{N}_{\mathrm{gr}}}{(\overline{N}_\mathrm{g}+\overline{N}_{\mathrm{gr}})(\overline{N}_\mathrm{r}+\overline{N}_{\mathrm{gr}})} \\ &= \overline{N}_{\mathrm{gr}} g_\mathrm{g}(0,0) g_\mathrm{r}(0,0)\end{aligned} \tag{5}$$

where $\overline{N}_\mathrm{g}, \overline{N}_\mathrm{r}$ and $\overline{N}_{\mathrm{gr}}$ are the average number of clusters containing green-labeled protein only, red-labeled protein only, or both green- and red-labeled proteins, respectively. The cluster density of co-localized red- and green-labeled proteins, $\mathrm{CD}_{\mathrm{gr}}$, can be extracted from the zero-lag amplitude of the cross-correlation function:

$$\mathrm{CD}_{\mathrm{gr}} = \frac{g_{\mathrm{gr}}(0,0)}{g_\mathrm{g}(0,0)g_\mathrm{r}(0,0)\pi\omega^2} = \frac{\overline{N}_{\mathrm{gr}}}{\pi\omega^2} \tag{6}$$

The fraction of each protein type that co-localizes with the other can be estimated by taking the ratios of CD values. The fraction of green-labeled protein clusters that contain red-labeled protein clusters is represented by $F(g/r)$ and correspondingly, the fraction of red-labeled protein clusters that contain green-labeled protein clusters is represented by $F(r/g)$:

$$F(g/r) = \frac{CD_{\mathrm{gr}}}{CD_\mathrm{g}} \quad F(r/g) = \frac{CD_{\mathrm{gr}}}{CD_\mathrm{r}} \tag{7}$$

Dynamic image correlation spectroscopy

Dynamic image correlation spectroscopy (DICS) is an extension of ICS and is used to measure dynamics of particle movements in solution and on cells. A cross-correlation function is obtained by correlating the image collected at one time with an image collected at a later time. This is done for an entire time series. The amplitude

of the cross-correlation function reveals the persistence of fluctuations at particular positions. Analysis of the rate and shape of the temporal decay of the amplitude of the cross-correlation function obtained this way provides information about the dynamic processes that give rise to changes in the position of fluorescence fluctuations from image to image. In these studies, the dynamic process of interest is the lateral diffusion of EGFR-GFP, AP-2 and caveolin-1; therefore, the decay of the amplitude of the cross-correlation function as a function of delay time, τ, is fit to a 3-parameter hyperbolic decay of the form:

$$g(0,0,\tau) = \frac{A}{1+\frac{\tau}{\tau_d}} + C \tag{8}$$

where A is the extrapolated amplitude of $g(0,0,\tau)$ when $\tau = 0$ and C is a constant that is added to allow for incomplete decay of correlations at long times due to immobile fluorescent particles and limited data records. From the fit we can obtain the diffusion time, τ_d, which enables us to calculate the diffusion coefficient, D, according to

$$D = \frac{\omega^2}{4\tau_d} \tag{9}$$

where ω is the $1/e^2$ radius of the focused laser beam.

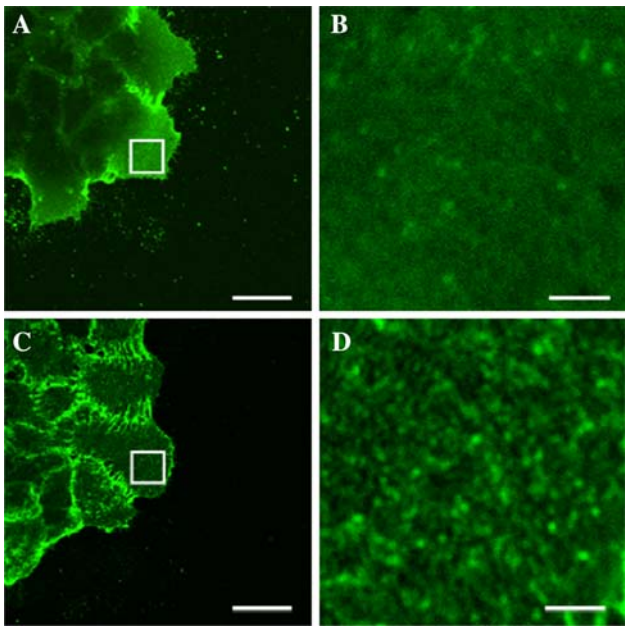

Fig. 1 Confocal images showing the distribution of EGFR at 37 and 4°C. A431 cells were paraformaldehyde fixed at 37°C (**a**, **b**) and 4°C (**c**, **d**) and immunofluorescently labeled for EGFR. Images **b** and **d** were collected from the regions indicated by the *white boxes* in **a** and **c**, respectively. *Scale bar* represents 32 μm in **a** and **c** and 3.2 μm in **b** and **d**

Results

The distribution of EGFR in cell membranes is temperature dependent

To determine the distribution of EGFR in cell membranes, A431 cells were fixed at 37, 23 and 4°C and immunofluorescently labeled with an antibody specific for EGFR. Figure 1a, c shows confocal images of such cells at 37 and 4°C, respectively. High magnification confocal images were collected from the periphery of cells as shown in Fig. 1b, d, collected from the boxed regions in Fig. 1a, c. Visual analysis of these images suggests that the distribution of EGFR is temperature-dependent. At 37°C, EGF receptors are diffusely distributed on the cell membrane, with few clusters being apparent. At 4°C, EGF receptors seem to be redistributed from a disperse population to an aggregated state consisting of large clusters of EGFR.

For each experimental condition, 120 high-magnification confocal images were collected and analyzed by ICS. The results are summarized in Table 1A as the average fluorescence intensity, CD and DA. As shown in Table 1A, the average fluorescence intensity does not significantly change at different temperatures. Because the intensities are essentially the same at the different temperatures, we infer that the number of EGF receptors expressed on the cell surface does not change as the temperature is varied, particularly at the periphery of the cell where the images are collected. Therefore, changes in the measured parameters, CD and DA, must arise from a rearrangement of EGFR rather than an increase or decrease in the number of detected EGFR. The average CD and DA do not change significantly as the temperature is lowered from 37 to 23°C; however, when the temperature is lowered to 4°C, there is a threefold decrease in the CD and a threefold increase in the DA, consistent with an aggregation of receptors into fewer and larger clusters. When the A431 cells were held at 4°C for various periods of time (15, 30, 45 and 60 min prior to being fixed) the measured CD and DA values were unchanged (Table 1B) indicating that aggregation of EGF receptors takes place within the first 15 min of cooling.

To test whether the aggregation of EGFR observed at 4°C on the surface of A431 cells is reversible when the temperature is raised back to 37°C, one dish of A431 cells was fixed using the paraformaldehyde protocol at 37°C, a second dish was fixed on ice at 4°C, and a third was cooled down to 4°C for 30 min, then warmed up to 37°C for 30 min prior to fixation. The calculated CD, DA and fluorescence intensity values for the three experimental conditions are shown in Table 1C. The CD of EGFR decreases by a factor of 3, as expected, when comparing 37 to 4°C conditions. When the cells were cooled down then

Table 1 Summary of the temperature effect on the distribution of EGFR on the surface of A431 cells

		I	CD	DA	*N*
A	37°C	20.7 ± 1.2	77.2 ± 5.0	0.53 ± 0.08	120
	23°C	22.0 ± 1.6	69.0 ± 5.3	0.63 ± 0.12	120
	4°C (15 min)	23.1 ± 0.8	26.7 ± 3.2	1.72 ± 0.21	120
B	4°C (30 min)	22.9 ± 1.5	27.0 ± 4.3	1.69 ± 0.22	70
	4°C (45 min)	22.1 ± 1.2	25.4 ± 3.1	1.73 ± 0.20	70
	4°C (60 min)	19.8 ± 1.5	23.6 ± 4.5	1.67 ± 0.29	70
C	37°C	21.7 ± 1.9	68.2 ± 7.5	0.69 ± 0.15	70
	4°C	20.0 ± 2.5	23.4 ± 5.2	1.59 ± 0.25	70
	4°C (30 min), 37°C (30 min)	17.9 ± 2.1	55.2 ± 6.2	0.82 ± 0.19	70

warmed up, the CD of EGFR increases by a factor of 2.3. These results indicate that EGF receptors aggregate into fewer, larger clusters at low temperature; however, they are not irreversibly trapped in this aggregated state since, as the temperature is increased, they redisperse into more, smaller clusters on the surface of A431 cells. Identical temperature-dependent experiments were carried out using A431 cells fixed using a methanol/acetone fixation procedure with similar outcomes indicating that aggregation of EGF receptors at low temperature is not an artifact of the specific fixation procedure.

Diffusion measurements of EGFR on cell membranes

To measure the dynamics of EGF receptors on the cell membrane, a glass coverslip containing COS-7 cells transfected with an EGFR-GFP fusion protein was introduced in a temperature stage and maintained in serum-free media. The temperature stage was set at 37°C and a series of 50 high-magnification, zoom10, confocal images were collected from the same region of the cell membrane at 8-s intervals and subjected to DICS analysis. The inset in Fig. 2a shows a transfected COS-7 cells from which one such time series was collected and the white box represents the region from which the images were collected. Figure 2a–d shows an example of such images and are shown as overlays of the image collected at time zero (shown in green) with itself and images collected 24, 160, and 400 s later (shown in red). The bright spots present in these images represent clusters of EGFR-GFP on the surface of living COS-7 cells. A total of 30 sets of 50 images were collected and subjected to DICS analysis to calculate the amplitude of the time-dependent cross-correlation function ($g(0,0,\tau)$) (Eq. 8). As the EGFR-GFP clusters move on the cell surface, the extent of co-localization between the image collected at time zero and images collected at later time points decreases. This is evident in the overlay images in Fig. 2b–d where the number of yellow spots decreases steadily. This movement of the clusters leads to a decrease in the amplitude of the cross-correlation function with time. Figure 2e shows this decay of the amplitude of the time-dependent cross-correlation function as a function of the delay time between the images, τ. Assuming that the cluster movement is by a diffusive process, the characteristic time for diffusion, τ_d, can be extracted by fitting to Eq. 8. In turn, we calculate the diffusion coefficient from: $D = \omega^2/4\tau_d$, where ω is the $1/e^2$ radius of the focused laser beam. The diffusion coefficient of EGFR-GFP clusters on the surface of live COS-7 cells at 37°C was calculated for 30 different time series on 30 different cells and the average value is 2.5×10^{-11} cm^2 s^{-1}.

The dynamics of EGFR clusters was also measured at 4°C. The inset in Fig. 3a shows a transfected COS-7 cells from which one such time series was collected. Figure 3a–d shows an example of high magnification confocal images taken from this time series and are shown as overlays of the image collected at time zero (shown in green) with itself and images collected 24, 160, and 400 s later (shown in red). Visual inspection of the overlaid high magnification confocal images indicates that EGFR-GFP clusters move very little at 4°C during the 400-s time period, since yellow spots persist throughout the time series. Figure 3e shows an example of the decay of the amplitude of the time dependent cross-correlation function as a function of the delay time between images, τ. The average diffusion coefficient of EGFR-GFP measured on 10 COS-7 cells at 4°C is 4.3×10^{-13} cm^2 s^{-1}, which is approximately two orders of magnitude slower than at 37°C.

Autocorrelation analysis of each confocal image in a time series provides CD and DA values as a function of real time. Figure 4a–c shows plots of average fluorescence intensity, CD and DA versus time, respectively, for one time series collected at 37°C. The average fluorescence intensity does not change significantly over the 400 s indicating that the area of the cell membrane is not photobleached during the process of image collection. The plots shown in Fig. 4b and c demonstrate that the number of EGFR-GFP clusters as well as the size of the clusters fluctuates with time around the mean value. The plots shown in Fig. 4d–f summarize the autocorrelation analysis of a corresponding time series collected at 4°C. The average fluorescence intensity does not change over 400 s indicating that the cell membrane is not photobleached during image collection and the CD and DA values change very little with time, consistent with the slow diffusion of EGFR-GFP clusters at 4°C.

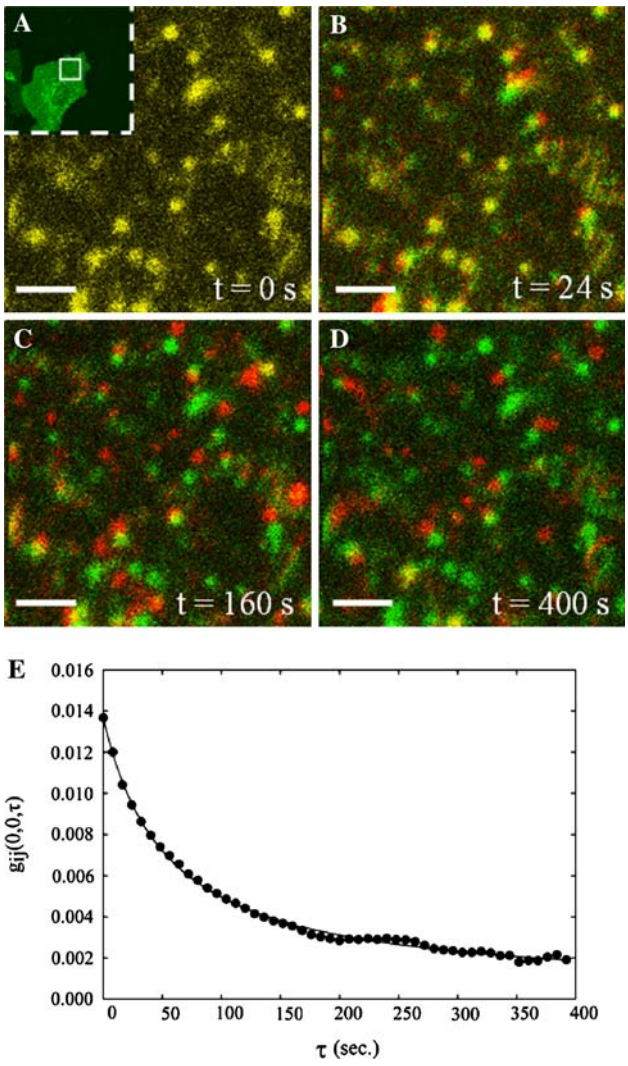

Fig. 2 EGFR clusters are dynamic at 37°C. COS-7 cells were transfected with EGFR-GFP. Forty-eight hours after the transfection, cells were inserted in a temperature stage set at 37°C. Fifty high magnification confocal images delayed by 8 s were collected from the same region of the cell membrane which is indicated by the *white box* in the insert of **a**. The images are shown as overlays of the image collected at 0 s (*green*) with itself (*red*) (**a**), with the image collected at 24 s (**b**), 160 s (**c**) and 400 s (**d**). *Bright spots* represent the spatial location of EGFR-GFP at 37°C. *Scale bars* represent 3.2 μm. These images were analyzed by DICS and the amplitude of the cross-correlation function is plotted as a function of delay time, $\tau(E)$. The smooth curve is the line of best fit to Eq. 8. Thirty such time series were collected from 30 different cells and the average diffusion coefficient of EGFR at 37°C was calculated to be 2.5×10^{-11} cm^2 s^{-1}

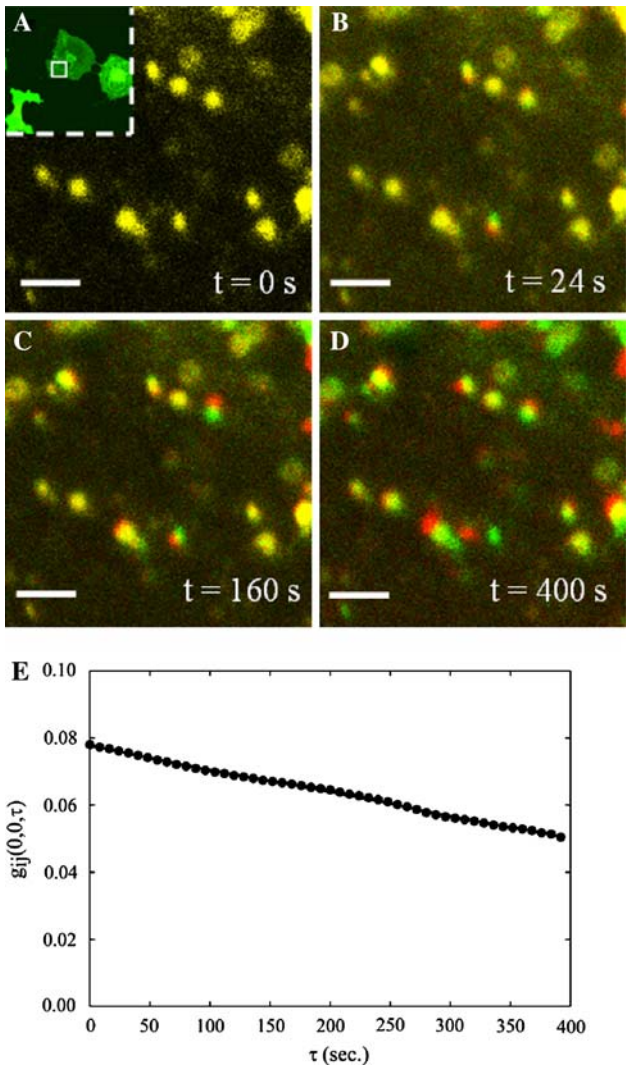

Fig. 3 EGFR clusters are immobile at 4°C. COS-7 cells were transfected with EGFR-GFP. Forty-eight hours after the transfection, cells were inserted in a temperature stage set at 4°C. Fifty high magnification confocal images delayed by 8 s were collected from the same region of the cell membrane which is indicated by the *white box* in the insert of **a**. The images are shown as overlays of the image collected at 0 s (*green*) with itself (*red*) (**a**), with the image collected at 24 s (**b**), 160 s (**c**) and 400 s (**d**). The *bright spots* represent the spatial location of EGFR-GFP at 4°C. *Scale bars* represent 3.2 μm. These images were analyzed by DICS and the amplitude of the cross-correlation function is plotted as a function of delay time, $\tau(E)$. The smooth curve is the line of best fit to Eq. 8. Ten such time series were collected from ten different cells and the average diffusion coefficient of EGFR at 4°C was calculated to be 4.3×10^{-13} cm^2 s^{-1}

Diffusion measurements of caveolin-1 and AP-2 on cell membranes

The diffusion coefficients of caveolin-1α, caveolin-1β and AP-2, all GFP-tagged, were measured on the plasma membrane of COS-7 cells at 37, 19 and 4°C. Cover slips containing transiently transfected COS-7 cells were placed in a temperature stage set to the desired temperature. For each experiment, a series of 50 high-magnification, zoom10, confocal images were collected from the same region of the cell membrane at 15-s intervals and subjected to DICS analysis. For each protein, at each experimental condition, ten time series were collected from ten different cells and the average diffusion coefficients are summarized

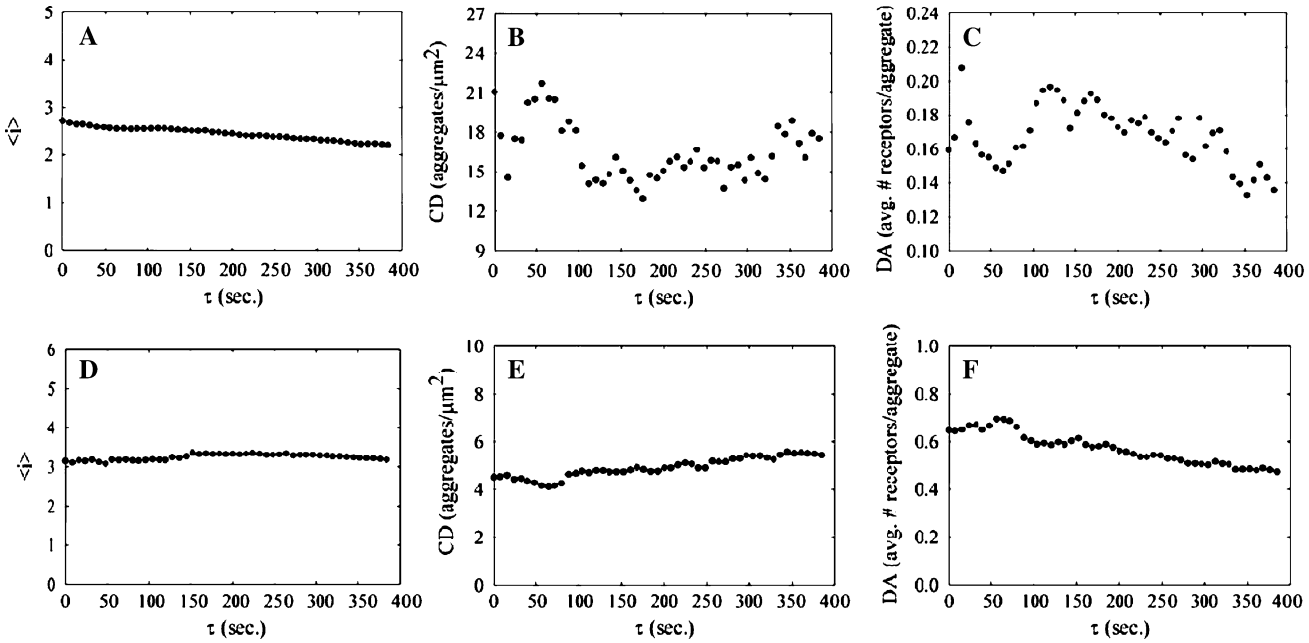

Fig. 4 Plots showing the effect of temperature on the number and size of EGFR clusters with time. COS-7 cells were transfected with EGFR-GFP. Forty-eight hours after the transfection cells were inserted in a temperature stage set at 37 or 4°C. High magnification confocal images were collected from the periphery of the cell as time series with 8-s intervals. These time series were analyzed by DICS. The autocorrelation results obtained for each image in the time series are plotted as average fluorescence intensity, CD and DA as a function of delay time τ, at 37°C (**a–c**) and 4°C (**d–f**). **a** and **d** show that the cell membrane was not photobleached during the collection of time series. **b**, **c** EGFR clusters are very dynamic at 37°C since the number (CD values) and size (DA values) of clusters vary with time. Very little variation in CD and DA values is observed at 4°C (**e**, **f**) indicating that EGFR clusters are almost immobile at low temperature

in Table 2. Our results indicate that temperature does not have a significant effect on the diffusion coefficients of AP-2 and caveolin-1α; however, caveolin-1β is highly dynamic at 37°C and virtually immobile at 4°C.

Co-localization studies show that EGF receptors are mostly present in membrane rafts and less in caveolae or clathrin-coated pits

Our results show that the diffusion of EGFR clusters and the variation in their number and size is dependent on temperature. More specifically, EGFR clusters are highly dynamic at 37°C and diffuse more than two orders of magnitude faster than at 4°C. These changes in dynamics with temperature are similar to those observed for GPI-anchored protein clusters (Nohe et al. 2006) and caveolin-1β clusters (Table 2). In contrast, there are virtually no changes in dynamics for clusters of AP-2 and caveolin-1α (Table 2). These comparisons suggest that the clusters of EGF receptors are in fact in membrane rafts and/or caveolae enriched in caveolin-1β. In separate sets of experiments, A431 cells were labeled with an antibody specific for EGFR and caveolin-1 (as a marker for caveolae) and for EGFR and AP-2 (as a marker for coated pits). In addition, cells were transfected with GFP-GL-GPI fusion protein (as a marker for rafts), fixed and labeled for EGFR. The degree of raft association of GL-GPI has been reported by Pralle et al. (2000) to be 76%. In each case, the EGF receptors were imaged in the red and the other proteins were imaged in green. Between 100 and 120 pairs of high-magnification confocal images were collected for the three sets of experiments and these were analyzed by ICCS to quantify the extent of co-localization of EGFR with the membrane domain-specific proteins. The ICCS results are summarized in Table 3 as the fraction of EGFR that co-localize with the other protein.

These results indicate that more than half of the EGFR population on the membrane of A431 cells is present in membrane rafts while only about 10% of the EGFR population is present in clathrin-coated pits. Two antibodies were available to label for caveolin-1, one specific for the α

Table 2 DICS results showing average diffusion coefficients for AP-2, caveolin-1α and caveolin-1β as a function of temperature

Diffusion coefficient, D ($\times 10^{-12}$ cm^2 s^{-1})			
	37°C	19°C	4°C
AP-2	2.0 ± 0.5	3.1 ± 0.8	1.7 ± 0.6
cav1-α	2.4 ± 0.6	3.0 ± 0.7	0.9 ± 0.2
cav1-β	5.0 ± 1.3	0.9 ± 0.2	0.0009 ± 0.0002

isoform and one recognizing both α and β isoforms. The ICCS results indicate that almost one fifth of EGF receptors co-localize with caveolin-1α which is similar to the fraction of EGFR that co-localize with caveolin-1$\alpha\beta$, indicating that the small fraction of EGF receptors that are present in caveolae are present in caveolae enriched in both caveolin-1 isoforms and little or no EGFR are in caveolae enriched in the β isoform. Addition of 37.5 ng/ml EGF for 10 min at 37°C leads to an increase in the number of EGFR in caveloae to about a third.

Discussion

The aim of this work was to study the distribution, dynamic properties and location of EGFR, a transmembrane protein, on the plasma membrane of fixed and live cells. This was achieved by utilizing a family of image-processing tools (ICS, ICCS and DICS) along with accepted cell biology techniques. These biophysical techniques enable us to extract quantitative information about protein distribution, diffusion coefficients and extent of co-localization from high-resolution fluorescence confocal images. The cell lines chosen for these studies, A431 and transiently transfected COS-7 cells, both overexpress EGFR. It is known that growth of human cancer cells is often dependent or facilitated by the over-expression of receptor tyrosine kinases (RTK), such as EGFR. Extensive research is going on involving studies of EGFR in A431 cells in order to better understand carcinoma cell growth and survival with the hope of discovering agents as anti-cancer drugs. For example, it has been shown that cholesterol depletion plays a role in modulating EGFR-mediated signaling. It has been reported that cholesterol deletion impairs receptor function and down stream signaling in the case of RTKs present in caveolae, like PDGFR, insulin receptor and TrkA, while it has an opposite effect on EGFR function, known to be in membrane rafts. We believe that our results provide information useful in many fields, in particular cancer research.

Changes in temperature from 37 to 4°C has a dramatic effect on the distribution of EGFR on the membrane of fixed A431 cells which could be observed qualitatively (Fig. 1) as well as quantitatively from ICS results (Table 1). At 37°C EGF receptors are dispersed in the membrane and as the temperature is cooled, they aggregate into fewer (Table 1A), larger clusters (Table 1A). It is important to note that the average fluorescence intensity remains unchanged at the two temperatures (Table 1), which indicates that the same number of EGF receptors is observed. This implies that the change in the number and size of clusters as a result of temperature variation must be due to a redistribution rather than presence of more or fewer EGF receptors. The aggregation of EGF receptors takes place within 15 min, since no further changes were observed as the cells were cooled for longer time periods (Table 1B). This aggregation is not an artifact of the fixation method since the same trend is observed using either the methanol/acetone (results not shown) or paraformaldehyde fixation protocols and is reversible (Table 1C). Visualized EGF receptors are present at the cell membrane and not intracellular, since the antibody used is specific for an extracellular region of EGFR and was added to fixed, non-permeabilized A431 cells.

To understand the effect of temperature on the size of EGFR clusters, degree of aggregation values calculated by ICS, which are defined as the average number of monomers per average number of protein clusters, were examined. These are not absolute values since they contain a proportionality constant, which depends on instrumental parameters. This constant can be calculated if parameters such as extinction coefficients, quantum yields, etc., are known or otherwise it can be estimated empirically as follows. When A431 cells were fixed at 37°C and immunofluorescently labeled for EGFR, the calculated CD value is 77 EGFR clusters/μm^2 (Table 1A). The surface area of A431 cells is reported to be 2,800 μm^2 (Haigler et al. 1979; van Belzen et al. 1988) meaning that 221,000 EGFR clusters are present on the surface of one A431 cell. It is also known that A431 cells express $\sim 2 \times 10^6$ EGF receptors (Kawamoto et al. 1983). Taken together, this information indicates that 9 EGFR monomers are present per cluster at 37°C on the surface of A431 cells. The results obtained at 23°C are not significantly different compared with the results obtained at 37°C. When A431 cells are fixed at 4°C and immunofluorescently labeled for EGFR, the CD value is 27 EGFR clusters/(μm^2 (Table 1A). Using the same surface area of A431 cells and total number of EGFR in A431 cells as above, a value of 26 EGFR monomers per cluster is calculated.

Table 3 ICCS results showing the extent of co-localization of EGFR with markers for membrane rafts (GPI), caveolae (cav1) and coated pits (AP-2), in the presence and absence of EGF

	F(EGFR/GPI)	F(EGFR/AP-2)	F(EGFR/cav1α)	F(EGFR/cav1$\alpha\beta$)
−EGF	0.58 ± 0.04	0.10 ± 0.01	0.17 ± 0.01	0.18 ± 0.02
+EGF	0.59 ± 0.05	0.28 ± 0.02	0.29 ± 0.02	0.27 ± 0.02

Interestingly, temperature has an opposite effect on the distribution of the platelet-derived growth factor β (PDGF-β) receptor, also an integral, transmembrane tyrosine kinase receptor (Wiseman 1995; Wiseman et al. 1997). Using ICS analysis, these studies showed that PDGF-β receptors disperse as the temperature is lowered from 37 to 4°C. Previous studies have also shown that PDGF-β receptors and EGF receptors do no co-localize on the plasma membrane of A431 cells (Srivastava 1998). This is consistent with the idea that the two receptor types must be present in different domains on the cell surface. There is also evidence, which shows that temperature does not affect the distribution of clathrin-associated adaptor protein 2 (AP-2), which functions in endocytosis at the plasma membrane (Brown 1998; Brown and Petersen 1998). These results, together with ours, indicate that changes in temperature do not have the same effect on all proteins present at the cell surface.

The plasma membrane of cells is a dynamic, heterogeneous mixture of proteins, lipids and other components. A change in temperature has an effect on the physical properties of membranes. At 37°C, the interior of the lipid bilayer is highly fluid, in the liquid crystal state, where the hydrocarbon chains of phospholipids are disordered. At low temperatures (4°C), some membrane lipids undergo transition to a gel-like solid, or crystalline state in which fatty acid tails are fully extended and highly ordered, and van der Waals interactions between adjacent chains are maximal (Voet and Voet 1995). It is possible that lipid phase changes caused by changes in temperature may induce reorganization of EGF receptors within the plane of the membrane; however, this cannot be the only effect since it should affect all membrane proteins in a similar fashion. The plasma membrane is organized into domains, such as clathrin-coated pits (Schmid 1997), caveolae (Harder and Simons 1997; Parton and Simons 1995; Parton and Richards 2003) and membrane rafts (Brown 1992; Harder and Simons 1997; Nichols and Lippincott-Schwartz 2001; Simons and Toomre 2000; Waugh et al. 2001), which have functions, such as receptor internalization and signaling. It is also possible that at different temperatures, EGF receptors are recruited from one domain type to another, or that temperature affects different domains differently. The aggregation of EGF receptors at low temperature is reversible (Table 1C). This indicates that the changes in the phospholipids bilayer that take place as a result of lowering the temperature do not trap EGF receptors permanently into particular domains on the cell surface. Rather, EGF receptors are free to disperse as the temperature is increased to 37°C and the lipid bilayer becomes more fluid.

The EGFR clusters are very dynamic in cell membranes at 37°C with an average diffusion coefficient of 2.5×10^{-11} $cm^2\ s^{-1}$. As the temperature is lowered to 4°C, EGFR clusters diffuse much slower with an average diffusion coefficient of 4.3×10^{-13} $cm^2\ s^{-1}$. These results, together with the distribution results outlined above indicate that lowering of the temperature causes an aggregation of EGF receptors and a decreased mobility of EGFR clusters on the surface of cells.

The lateral diffusion of EGF receptors on the surface of different cell lines (Benveniste et al. 1988; Livneh et al. 1986; Rees et al. 1984; Schlessinger et al. 1983; Zidovetzki et al. 1981) has been studied previously using FPR. The diffusion coefficients measured at 37°C by FPR studies are more than an order of magnitude faster than the diffusion coefficients measured by DICS. It is important to note that the dynamic processes measured by DICS are limited by the rate of acquisition of images and by the size of the laser beam. This means that if proteins move too fast, 10^{-10} $cm^2\ s^{-1}$ or faster, the correlation between two adjacent images will be gone. Since clusters of proteins diffuse more than an order of magnitude slower than single molecules, DICS is a suitable method to measure their diffusion. On the other hand, FPR measures the diffusion coefficient of single proteins, which is fast, while protein clusters appear immobile. FPR and DICS were used to measure the diffusion coefficient of transferrin receptors (TfR) at room temperature (Srivastava 1998; Srivastava and Petersen 1998). The value obtained from FPR measurements was more than two orders of magnitude faster than the value obtained from DICS measurements using the same cell line and method of labeling. These observations confirm that the dynamics of single molecules differ from the dynamics of clusters of the same molecules.

The diffusion coefficient of EGFR clusters measured by DICS is an average of all types of diffusion (random, restricted, directed, etc.) that this receptor may undergo in the cell membrane. Using SPT and EGF bound to gold particles, Kusumi et al. (1993) showed that, at 37°C, the majority of EGF receptors undergo either restricted or simple diffusion, while a smaller fraction is stationary or experiences directed motion. The diffusion coefficient of freely diffusing proteins in a plasma membrane is theoretically expected to be $\sim 10^{-9}$ $cm^2\ s^{-1}$. Most membrane proteins exhibit slower diffusion, which is due to interactions with the cytoskeleton, cytoplasmic constituents, interactions with other membrane proteins or entrapment in domains formed by the cytoskeleton meshwork. EGF receptors have been shown to interact directly with actin microfilaments (den Hartigh et al. 1992; Rijken et al. 1991; van Bergen en Henegouwen et al. 1992), which could explain the slower diffusion of EGFR as compared to expected free Brownian diffusion on cell membranes. Studies have shown that F-actin depolymerization increases the diffusion coefficient of EGFR (Orr et al. 2005).

These studies contradict previous results that showed that large deletions in the cytoplasmic domain of EGFR, which would eliminate the amino acid residues that have been shown to interact with actin, do not affect the receptor's lateral mobility on the cell surface (Benveniste et al. 1988).

The diffusion coefficient of proteins specific for three types of membrane domains have been measured in live cells at different temperatures: a GPI-anchored protein (Nohe et al. 2006), which has been shown to be associated with membrane rafts to 76% (Pralle et al. 2000); both isoforms of caveolin-1, α and β (Table 2) which are known to be present in caveolae; and AP-2 (Table 2), which is an adaptor protein present in clathrin-coated pits. These results indicate that the diffusion of the GPI-anchored protein and caveolin-1β is affected by changes in temperature: these proteins are dynamic at 37°C and almost immobile at 4°C. In contrast, the diffusion of caveolin-1α and AP-2 is not significantly different at 37°C compared to 4°C. Our results are in agreement with FRAP results (Kenworthy et al. 2004) that also show that the same GPI-anchored protein diffuses much slower when the temperature is reduced. Since the diffusion of EGFR clusters is also temperature dependent, we wanted to investigate whether EGF receptors are localized in membrane rafts or cavelolae enriched in the caveolin-1β isoform by performing co-localization studies. Our results indicate that more than half of the EGFR population co-localizes with the GPI-anchored protein and addition of 37.5 ng/ml EGF at 37°C has no significant effect on the extent of co-localization (Table 3). Our results are in close agreement with previous work by Ringerike et al. (2002) who used electron microscopy and antibodies specific for EGFR and placental alkaline phosphatase (PLAP), a raft-localized GPI-anchored protein. This study showed that 40% of EGF receptors present on the surface of A431 cells localize within rafts and that this percentage is not affected by addition of gold-labeled EGF (Ringerike et al. 2002). (Other studies have shown that EGF receptors are present in membrane rafts containing the ganglioside GM1 (Zurita et al. 2004) and were only present in rafts that contained significant levels of both inner and outer leaflet lipds (Pike et al. 2005).

Our co-localization results show that about 20% of the EGFR population co-localizes with caveolin-1 and addition of EGF at 37°C leads to slight increase in the number of EGFR present in caveolae to about 30% (Table 3). The presence of EGFR in caveolae has been studied previously. Experiments where caveolin-enriched membrane domains were isolated by fractionation showed that 40–60% of EGF receptors on the surface of cells are present in caveolae (Mineo et al. 1999). Arguments have been made to the effect that these membrane fractions contain caveolae and could also be contaminated by non-caveolar membrane fragments (Waugh et al. 1999). Studies using electron microscopy and gold-labeled antibodies specific for EGFR and caveolin-1 showed that only 7% of the total number of EGFR on the plasma membrane of A431 cells was within caveolae (Ringerike et al. 2002). They also reported that no change was observed in the EGFR distribution upon incubation with EGF at 4°C. This study did not distinguish between the two caveolin-1 isoforms. Finally, about 10% of the EGFR population co-localizes with AP-2 and addition of EGF leads to an increase of the number of EGFR in clathrin-coated pits to about 30% (Table 3).

In conclusion, our studies demonstrate that EGF receptors are distributed as clusters on the surface of A431 cells and this distribution is affected by changes in temperature. Lowering the temperature from 37 to 4°C not only leads to an aggregation of EGFR but also to a decrease in the diffusion coefficient of this protein in the cell membrane. Finally, we showed that the dynamic behavior of EGFR is similar to a GPI-anchored protein known to be present in membrane rafts and that EGFR co-localizes to a high extent with this GPI-anchored protein indicating that the majority of the EGFR population on the surface of A431 cells is present in membrane rafts in the presence and absence of EGF.

It is tempting to speculate that the distribution of EGFR among domains is dynamic, that is the receptors continually shuffle from one domain to the other, perhaps in a directional manner that depends on stimulation. In steady state, the majority of the receptors are in rafts, but as they are exposed to EGF, the proportion in caveolae and coated pits increases. This could make sense if the rafts serve to optimize EGFR-EGFR interactions, caveolae serve as signaling complexes and coated pits as recycling centers. This pattern of behavior may be unique to EGFR and may not be applicable for PDGFR or TfR since they do not co-localize.

References

Benveniste M, Livneh E, Schlessinger J, Kam Z (1988) Overexpression of epidermal growth factor receptor in NIH-3T3-transfected cells slows its lateral diffusion and rate of endocytosis. J Cell Biol 106:1903–1909

Brown DA (1992) Interactions between GPI-anchored proteins and membrane lipids. Trends Cell Biol 2:338–343

Brown CM (1998) Distribution and co-localization of plasma membrane associated proteins. The University of Western Ontario. Thesis/dissertation

Brown CM, Petersen NO (1998) An image correlation analysis of the distribution of clathrin associated adaptor protein (AP-2) at the plasma membrane. J Cell Sci 111:271–281

Carpentier JL, Gorden P, Anderson RG, Goldstein JL, Brown MS, Cohen S, Orci L (1982) Co-localization of 125I-epidermal growth factor and ferritin-low density lipoprotein in coated pits: a quantitative electron microscopic study in normal and mutant human fibroblasts. J Cell Biol 95:73–77

Couet J, Sargiacomo M, Lisanti MP (1997) Interaction of a receptor tyrosine kinase, EGF-R, with caveolins. Caveolin binding negatively regulates tyrosine and serine/threonine kinase activities. J Biol Chem 272:30429–30438

den Hartigh JC, van Bergen en Henegouwen PM, Verkleij AJ, Boonstra J (1992) The EGF receptor is an actin-binding protein. J Cell Biol 119:349–355

Fiedler K, Kobayashi T, Kurzchalia TV, Simons K (1993) Glycosphingolipid-enriched, detergent-insoluble complexes in protein sorting in epithelial cells. Biochemistry 32:6365–6373

Goldstein JL, Brown MS, Anderson RG, Russell DW, Schneider WJ (1985) Receptor-mediated endocytosis: concepts emerging from the LDL receptor system. Annu Rev Cell Biol 1:1–39

Gorden P, Carpentier JL, Cohen S, Orci L (1978) Epidermal growth factor: morphological demonstration of binding, internalization, and lysosomal association in human fibroblasts. Proc Natl Acad Sci USA 75:5025–5029

Haigler HT, McKanna JA, Cohen S (1979) Direct visualization of the binding and internalization of a ferritin conjugate of epidermal growth factor in human carcinoma cells A-431. J Cell Biol 81:382–395

Hanover JA, Willingham MC, Pastan I (1984) Kinetics of transit of transferrin and epidermal growth factor through clathrin-coated membranes. Cell 39:283–293

Harder T, Simons K (1997) Caveolae, DIGs, and the dynamics of sphingolipid-cholesterol microdomains. Curr Opin Cell Biol 9:534–542

Hopkins CR, Miller K, Beardmore JM (1985) Receptor-mediated endocytosis of transferrin and epidermal growth factor receptors: a comparison of constitutive and ligand-induced uptake. J Cell Sci Suppl 3:173–186

Kawamoto T, Sato JD, Le A, Polikoff J, Sato GH, Mendelsohn J (1983) Growth stimulation of A431 cells by epidermal growth factor: identification of high-affinity receptors for epidermal growth factor by an anti-receptor monoclonal antibody. Proc Natl Acad Sci USA 80:1337–1341

Kenworthy AK, Nichols BJ, Remmert CL, Hendrix GM, Kumar M, Zimmerberg J, Lippincott-Schwartz J (2004) Dynamics of putative raft-associated proteins at the cell surface. J Cell Biol 165:735–746

Kusumi A, Sako Y, Yamamoto M (1993) Confined lateral diffusion of membrane receptors as studied by single particle tracking (nanovid microscopy): effects of calcium-induced differentiation in cultured epithelial cells. Biophys J 65:2021–2040

Liu P, Ying Y, Ko YG, Anderson RG (1996) Localization of platelet-derived growth factor-stimulated phosphorylation cascade to caveolae. J Biol Chem 271:10299–10303

Livneh E, Benefits M, Prywes R, Felder S, Kam Z, Schlessinger J (1986) Large deletions in the cytoplasmic kinase domain of the epidermal growth factor receptor do not affect its laternal mobility. J Cell Biol 103:327–331

Metzger H (1992) Transmembrane signaling: the joy of aggregation. J Immunol 149:1477–1487

Mineo C, James GL, Smart EJ, Anderson RG (1996) Localization of epidermal growth factor-stimulated Ras/Raf-1 interaction to caveolae membrane. J Biol Chem 271:11930–11935

Mineo C, Gill GN, Anderson RG (1999) Regulated migration of epidermal growth factor receptor from caveolae. J Biol Chem 274:30636–30643

Nagy P, Arndt-Jovin DJ, Jovin TM (2003) Small interfering RNAs suppress the expression of endogenous and GFP-fused epidermal growth factor receptor (erbB1) and induce apoptosis in erbB1-overexpressing cells. Exp Cell Res 285:39–49

Nichols BJ, Lippincott-Schwartz J (2001) Endocytosis without clathrin coats. Trends Cell Biol 11:406–412

Nohe A, Keating E, Petersen NO (2006) Dynamics of GPI-anchored proteins on the surface of living cells. Nanomedicine 2:1–7

Orr G, Hu D, Ozcelik S, Opresko LK, Wiley HS, Colson SD (2005) Cholesterol dictates the freedom of EGF receptors and HER2 in the plane of the membrane. Biophys J 89:1362–1373

Parton RG, Richards AA (2003) Lipid rafts and caveolae as portals for endocytosis: new insights and common mechanisms. Traffic 4:724–738

Parton RG, Simons K (1995) Digging into caveolae. Science 269:1398–1399

Petersen NO (1986) Scanning fluorescence correlation spectroscopy: I. Theory and simulation of aggregation measurements. Biophys J 49:809–815

Petersen NO, Hoddelius PL, Wiseman PW, Seger O, Magnusson KE (1993) Quantitation of membrane receptor distributions by image correlation spectroscopy: concept and application. Biophys J 65:1135–1146

Petersen NO, Brown C, Kaminski A, Rocheleau JV, Srivastava M, Wiseman PW (1998) Analysis of membrane protein cluster densities and sizes in situ by image correlation spectroscopy. Faraday Discuss 111:289

Pike LJ, Miller JM (1998) Cholesterol depletion delocalizes phosphatidylinositol bisphosphate and inhibits hormone-stimulated phosphatidylinositol turnover. J Biol Chem 273:22298–22304

Pike LJ, Han X, Gross RW (2005) Epidermal growth factor receptors are localized to lipid rafts that contain a balance of inner and outer leaflet lipids: a shotgun lipidomics study. J Biol Chem 280:26796–26804

Pralle A, Keller P, Florin EL, Simons K, Horber JK (2000) Sphingolipid-cholesterol rafts diffuse as small entities in the plasma membrane of mammalian cells. J Cell Biol 148:997–1008

Prinetti A, Chigorno V, Tettamanti G, Sonnino S (2000) Sphingolipid-enriched membrane domains from rat cerebellar granule cells differentiated in culture: a compositional study. J Biol Chem 275:11658–11665

Rees AR, Gregoriou M, Johnson P, Garland PB (1984) High affinity epidermal growth factor receptors on the surface of A431 cells have restricted lateral diffusion. EMBO J 3:1843–1847

Rijken PJ, Hage WJ, van Bergen en Henegouwen PM, Verkleij AJ, Boonstra J (1991) Epidermal growth factor induces rapid reorganization of the actin microfilament system in human A431 cells. J Cell Sci 100(Pt 3):491–499

Ringerike T, Blystad FD, Levy FO, Madshus IM, Stang E (2002) Cholesterol is important in control of EGF receptor kinase activity but EGF receptors are not concentrated in caveolae. J Cell Sci 115:1331–1340

Robinson MS (1987) 100-kD coated vesicle proteins: molecular heterogeneity and intracellular distribution studied with monoclonal antibodies. J Cell Biol 104:887–895

Rocheleau JV, Petersen NO (2000) Sendai virus binds to a dispersed population of NBD-GD1a. Biosci Rep 20:139–155

Schlessinger J (1986) Allosteric regulation of the epidermal growth factor receptor kinase. J Cell Biol 103:2067–2072

Schlessinger J, Schreiber AB, Levi A, Lax I, Libermann T, Yarden Y (1983) Regulation of cell proliferation by epidermal growth factor. CRC Crit Rev Biochem 14:93–111

Schmid SL (1997) Clathrin-coated vesicle formation and protein sorting: an integrated process. Annu Rev Biochem 66:511–548

Sheets ED, Simson R, Jacobson K (1995) New insights into membrane dynamics from the analysis of cell surface interactions by physical methods. Curr Opin Cell Biol 7:707–714

Simons K, Toomre D (2000) Lipid rafts and signal transduction. Nat Rev Mol Cell Biol 1:31–39

Sorkin A, Mazzotti M, Sorkina T, Scotto L, Beguinot L (1996) Epidermal growth factor receptor interaction with clathrin

adaptors is mediated by the Tyr974-containing internalization motif. J Biol Chem 271:13377–13384
Srivastava M (1998) Image cross-correlation spectroscopy: development and applications on living and fixed cells. The University of Western Ontario. Thesis/dissertation
Srivastava M, Petersen NO (1996) Image cross-correlation spectroscopy: a new experimental biophysical approach to measurements of slow diffusion of fluorescent molecules. Meth Cell Sci 18:47
Srivastava M, Petersen NO (1998) Diffusion of transferrin receptor clusters. Biophys Chem 75:201–211
St Pierre PR, Petersen NO (1992) Average density and size of microclusters of epidermal growth factor receptors on A431 cells. Biochemistry 31:2459–2463
Ullrich A, Coussens L, Hayflick JS, Dull TJ, Gray A, Tam AW, Lee J, Yarden Y, Libermann TA, Schlessinger J (1984) Human epidermal growth factor receptor cDNA sequence and aberrant expression of the amplified gene in A431 epidermoid carcinoma cells. Nature 309:418–425
van Belzen N, Rijken PJ, Hage WJ, de Laat SW, Verkleij AJ, Boonstra J (1988) Direct visualization and quantitative analysis of epidermal growth factor-induced receptor clustering. J Cell Physiol 134:413–420
van Bergen en Henegouwen PM, den Hartigh JC, Romeyn P, Verkleij AJ, Boonstra J (1992) The epidermal growth factor receptor is associated with actin filaments. Exp Cell Res 199:90–97
Voet D, Voet JG (1995) Biochemistry. Wiley, New York, pp 288–289
Waugh MG, Lawson D, Hsuan JJ (1999) Epidermal growth factor receptor activation is localized within low-buoyant density, non-caveolar membrane domains. Biochem J 337(Pt 3):591–597
Waugh MG, Minogue S, Anderson JS, dos Santos M, Hsuan JJ (2001) Signalling and non-caveolar rafts. Biochem Soc Trans 29:509–512
Wiseman PW (1995) Image correlation spectroscopy development and application to studies of PDGF receptor distribution. The University of Western Ontario. Thesis/dissertation
Wiseman PW, Petersen NO (1999) Image correlation spectroscopy: II. Optimization for ultrasensitive detection of preexisting platelet-derived growth factor-beta receptor oligomers on intact cells. Biophys J 76:963–977
Wiseman PW, Hoddelius P, Petersen NO, Magnusson KE (1997) Aggregation of PDGF-beta receptors in human skin fibroblasts: characterization by image correlation spectroscopy (ICS). FEBS Lett 401:43–48
Zidovetzki R, Yarden Y, Schlessinger J, Jovin TM (1981) Rotational diffusion of epidermal growth factor complexed to cell surface receptors reflects rapid microaggregation and endocytosis of occupied receptors. Proc Natl Acad Sci USA 78:6981–6985
Zurita AR, Crespo PM, Koritschoner NP, Daniotti JL (2004) Membrane distribution of epidermal growth factor receptors in cells expressing different gangliosides. Eur J Biochem 271:2428–2437